Supplementary Figure 1

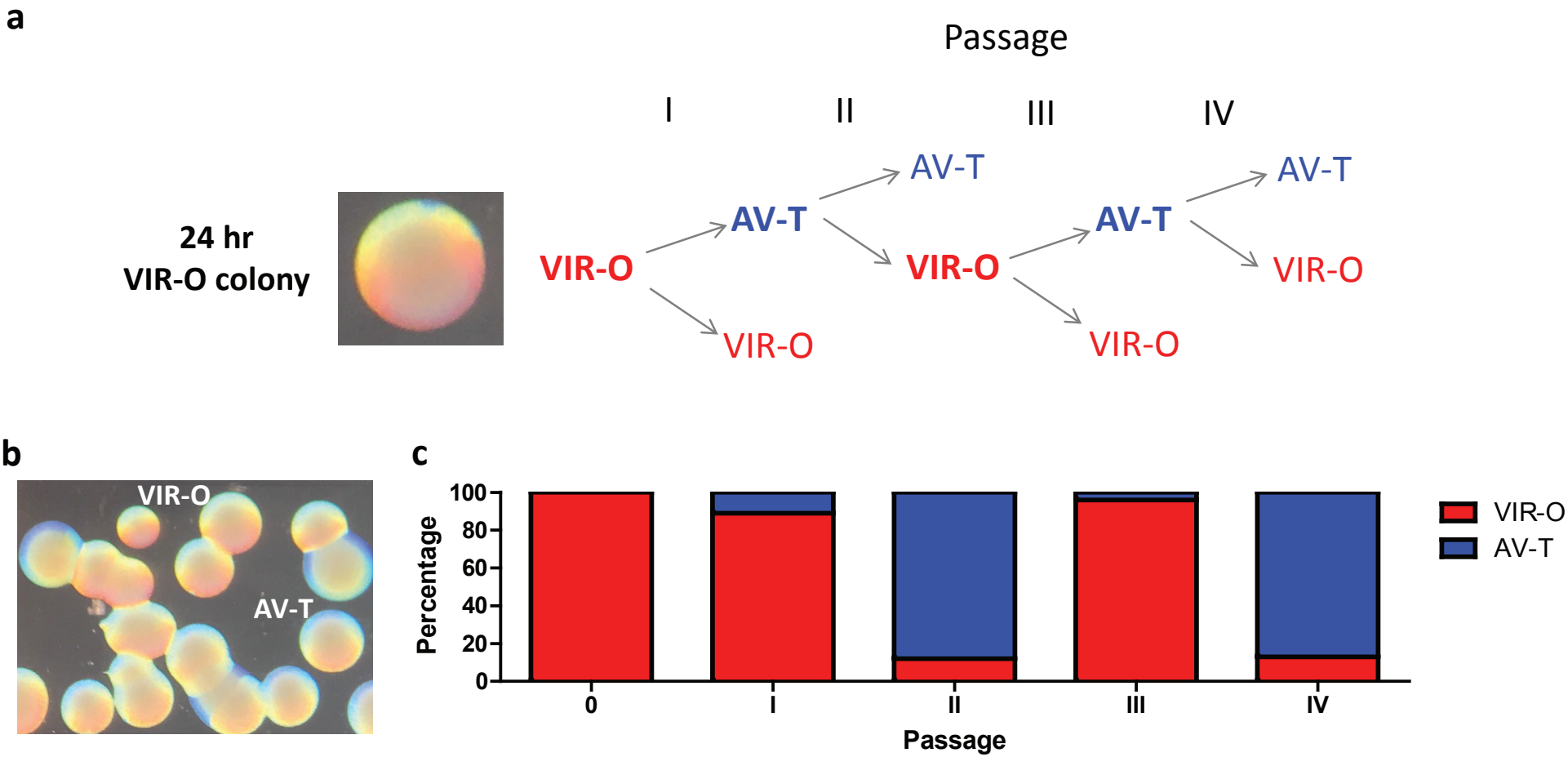

Supplementary Fig. 1. Switching frequencies between VIR-O (red) and AV-T (blue) from a 24 hour colony. (a), A single representative VIR-O colony is shown after 24 hours of growth on a 0.5X LB agar plate. At this time, three replicate VIR-O colonies were resuspended and dilutions were plated to assess the frequency of cells that switched to AV-T **(b, c)**. After 24 hours of growth, the switching frequency of three replicate AV-T colonies to VIR-O was determined as described above **(c)**. This was then sequentially repeated two additional times.

Supplementary Figure 2

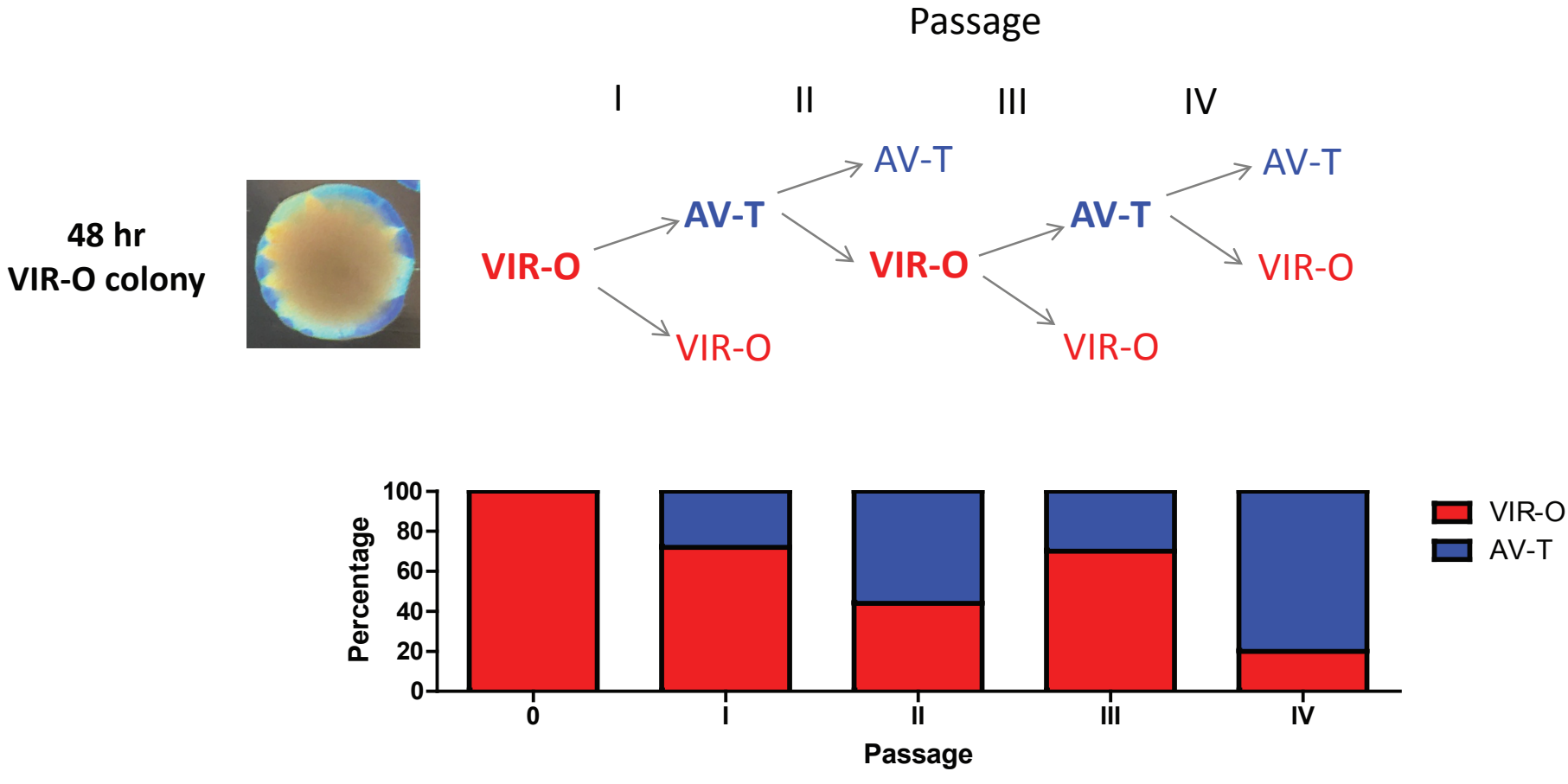

Supplementary Fig. 2. Switching frequencies between VIR-O (red) and AV-T (blue) from a 48 hour colony. A representative 48 hour VIR-O colony is shown. Note the high degree of AV-T sectors that have formed. Switching frequencies were determined as described in Supplemental Fig. 1 using three replicate colonies for each condition.

Supplementary Figure 3

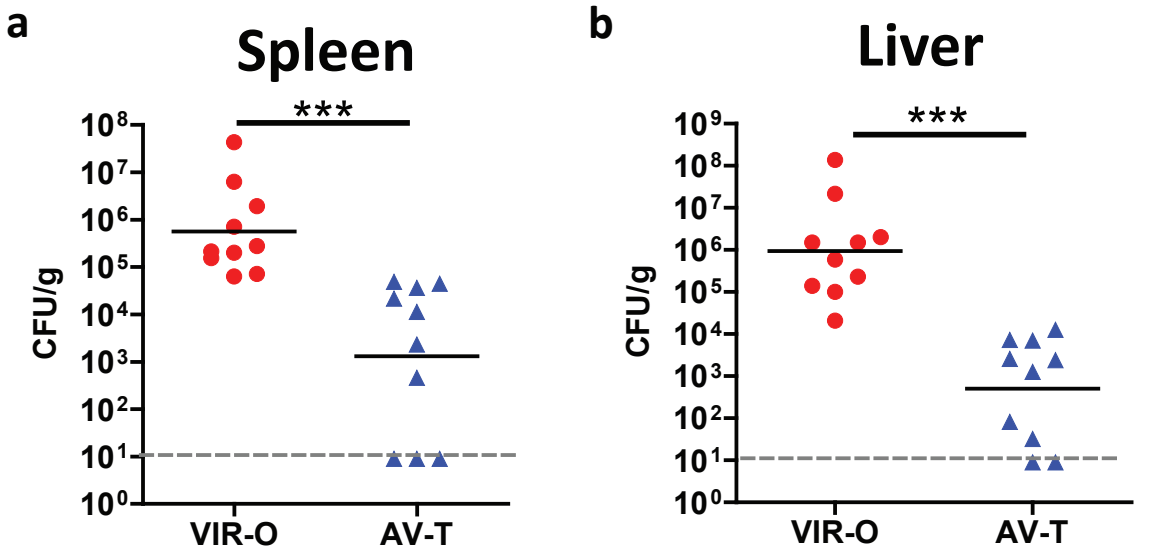

Supplementary Fig. 3. A highly virulent opaque (VIR-O) population is responsible for systemic infection in mice. Mice were infected intranasally with VIR-O (red) or AV-T (blue) strains (n=5/ group). Presented data were pooled from two separate experiments and repeated at least 10 times. At 24 hours post-infection, **(a)** spleens and **(b)** livers were harvested and plated for colony forming unit enumeration. Dashed lines represent the limit of detection. Error bars represent geometric mean and significance was determined using a two-tailed Mann-Whitney test (***$p < 0.0005$).

Supplementary Figure 4

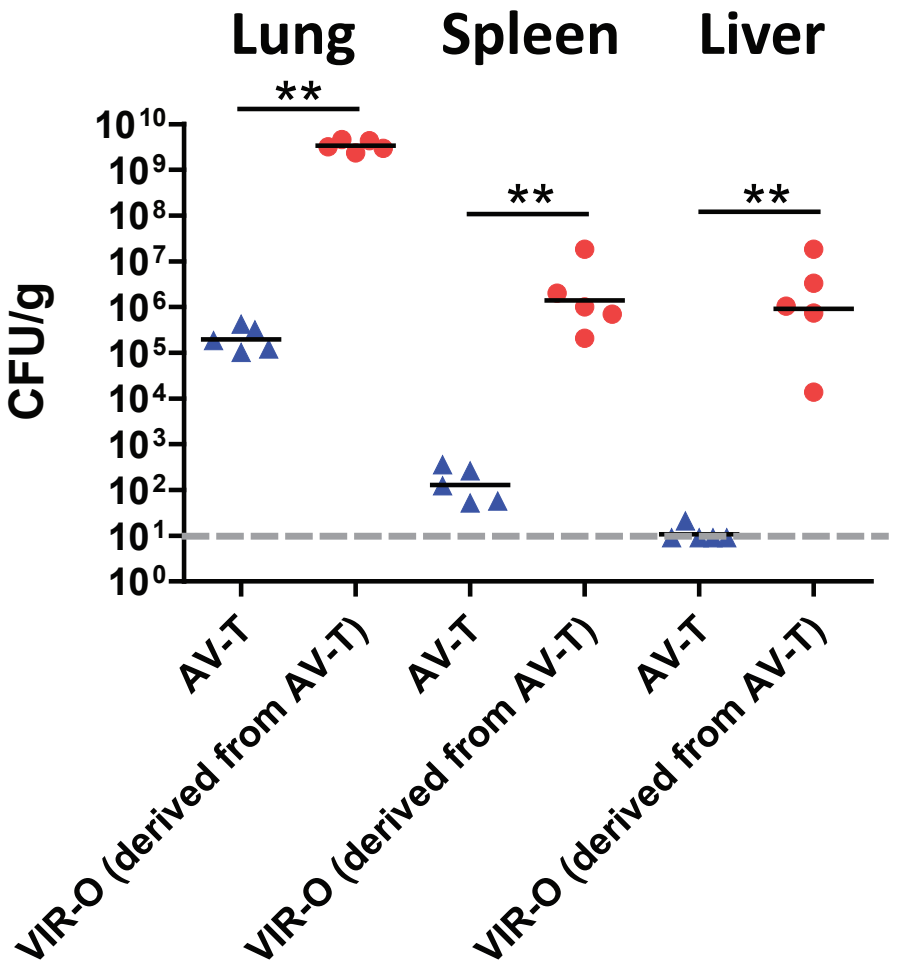

Supplementary Fig. 4. VIR-O cells derived from AV-T colonies regain virulence in mice. Mice were infected intranasally with VIR-O (red) or AV-T (blue) strains (n=5/ group). This experiment was repeated two times. At 24 hours post-infection, organs were harvested and plated for colony forming unit enumeration. Dashed lines represent the limit of detection. Error bars represent geometric mean and significance was determined using a two-tailed Mann-Whitney test (**$p < 0.005$).

Supplementary Figure 5

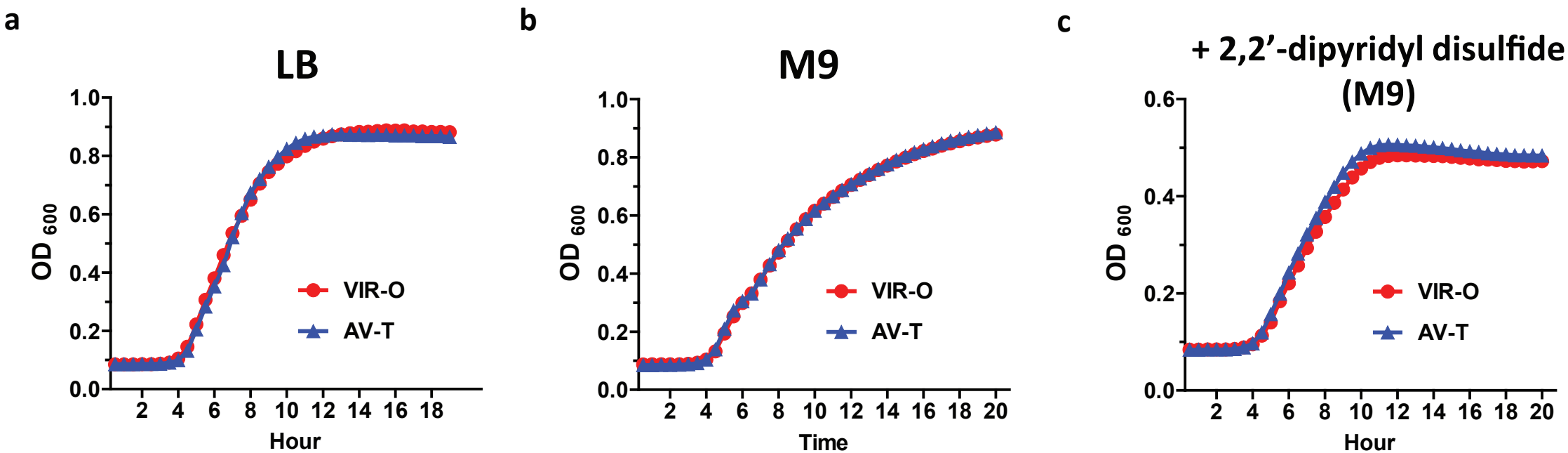

Supplementary Fig. 5. Growth kinetics of the VIR-O and AV-T in rich or defined media. VIR-O (red) or AV-T (blue) strains were grown in **(a)** LB, **(b)** M9 supplemented with 0.2% casamino acids, and **(c)** M9 supplemented with 0.2% casamino acids and the iron chelator, 2,2'-dipyridyl disulfide (156 µM). Cultures were incubated at 37°C with aeration in a Biotek Synergy Mx plate reader and OD_{600} was measured each 30min for 20 hours. All values were determined using three replicates for each condition.

Supplementary Figure 6

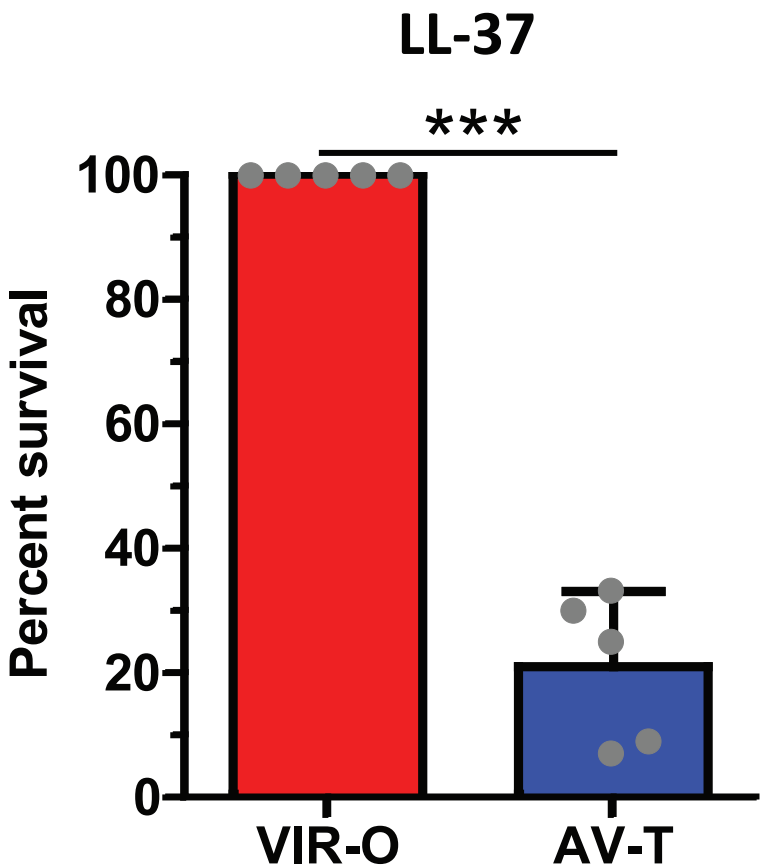

Supplementary Fig. 6. VIR-O is resistant to the human antimicrobial peptide LL-37. VIR-O (red) or AV-T (blue) was treated with human antimicrobial peptide LL-37 for 1 hour, and percent survival relative to VIR-O was calculated. Error bars represent standard deviation of the mean and Student's two-tailed *t*-test (***$p < 0.0005$). The reported values represent the mean of five replicates.

Supplementary Figure 7

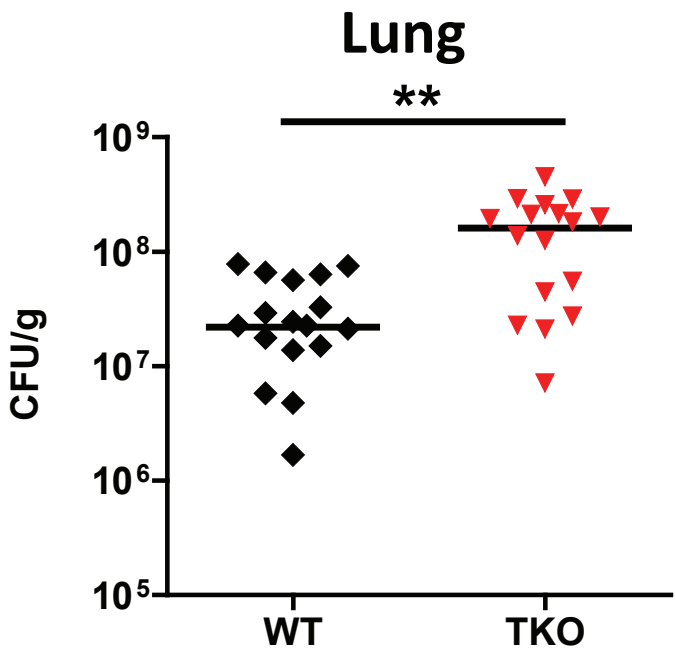

Supplementary Fig. 7. Triple knockout mice lacking antimicrobials exhibit increased bacterial levels during AV-T infection. Wild-type (WT, black) or triple knockout (TKO; red) mice lacking the gp91 subunit of the NADPH oxidase, lysozyme and CRAMP were infected with AV-T (n=4 to 8/ group). Presented data were pooled from three separate experiments and repeated at least 5 times. At 8 hours post-infection, lungs were harvested and plated for colony forming unit enumeration. Error bars represent geometric mean and significance was determined using a two-tailed Mann-Whitney test (**$p < 0.005$).

Supplementary Figure 8

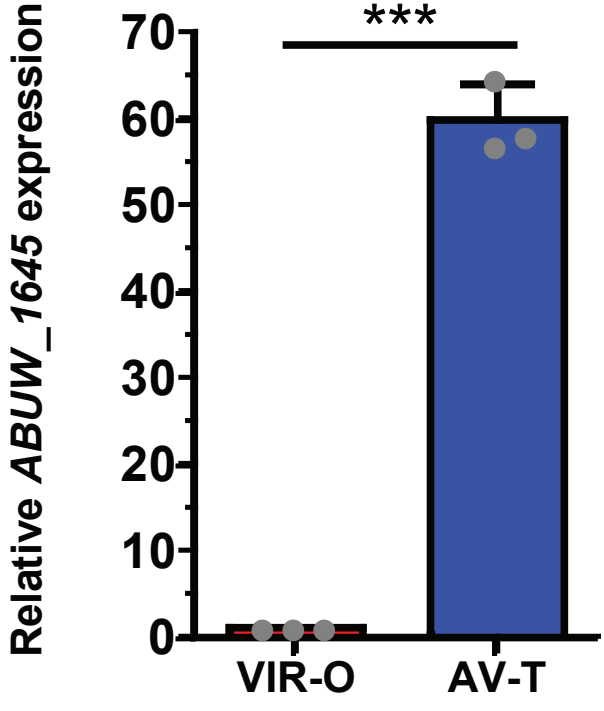

Supplementary Fig. 8. AV-T cells express higher levels of *ABUW_1645*. RNA was harvested from AV-T and VIR-O cultures and used for quantitative real time analysis of *ABUW_1645* expression relative to the *clpX* gene. Error bars represent standard deviation of the mean for 3 replicates and *p*-values were determined using Student's two-tailed *t*-test (***$p < 0.005$).

Supplementary Figure 9

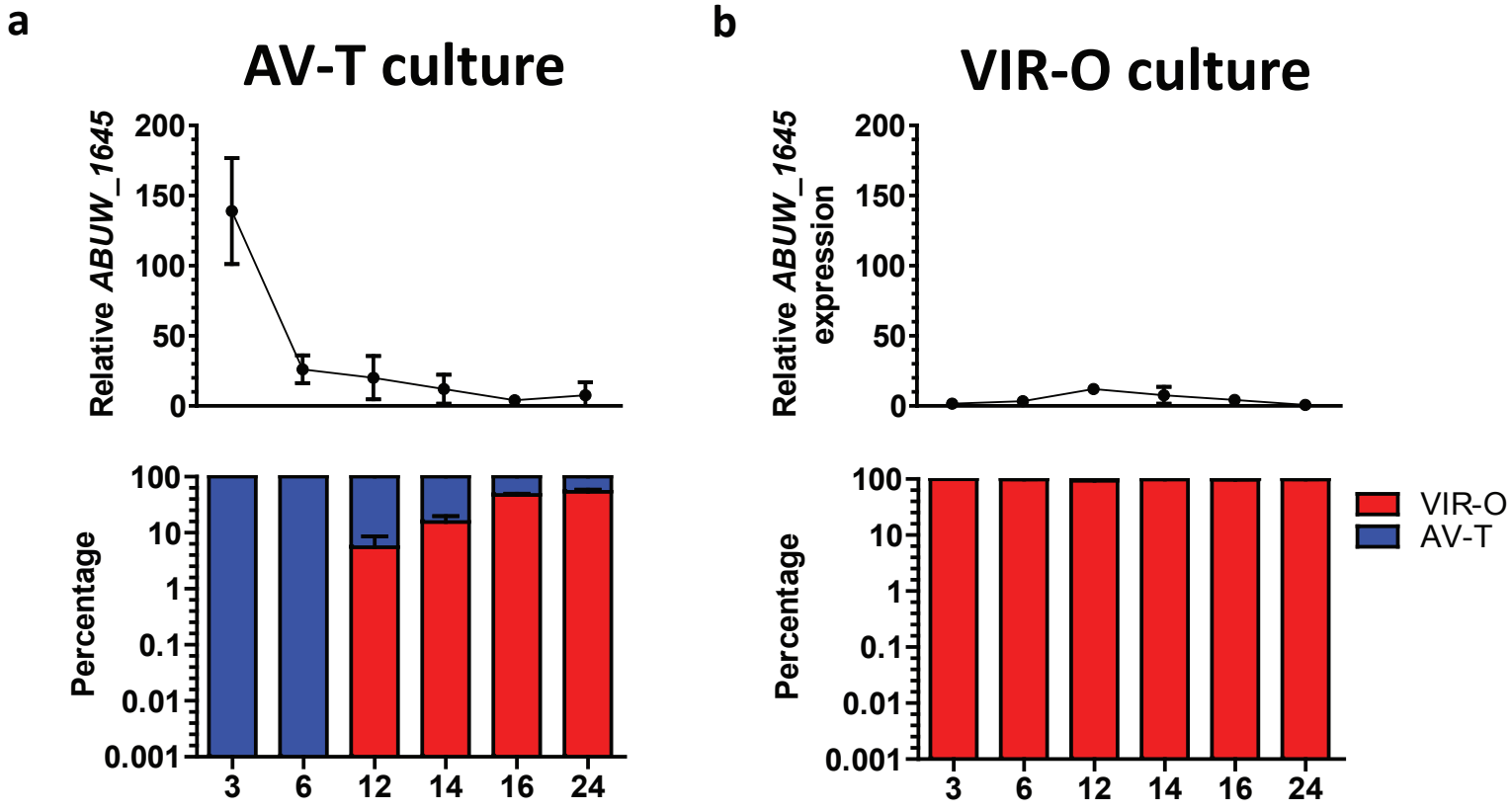

Supplementary Fig. 9. ***ABUW_1645*** **expression correlates with phenotypic VIR-O and AV-T switch.** RNA was harvested from **(a)** AV-T and **(b)** VIR-O cultures over the course of 24 hours and used for quantitative real time analysis of *ABUW_1645* expression relative to the housekeeping 16s rRNA. At each time point, cultures were plated to assess for the percentage of VIR-O and AV-T cells present. Values represent the mean of three replicates and error bars represent standard deviations.

Supplementary Figure 10

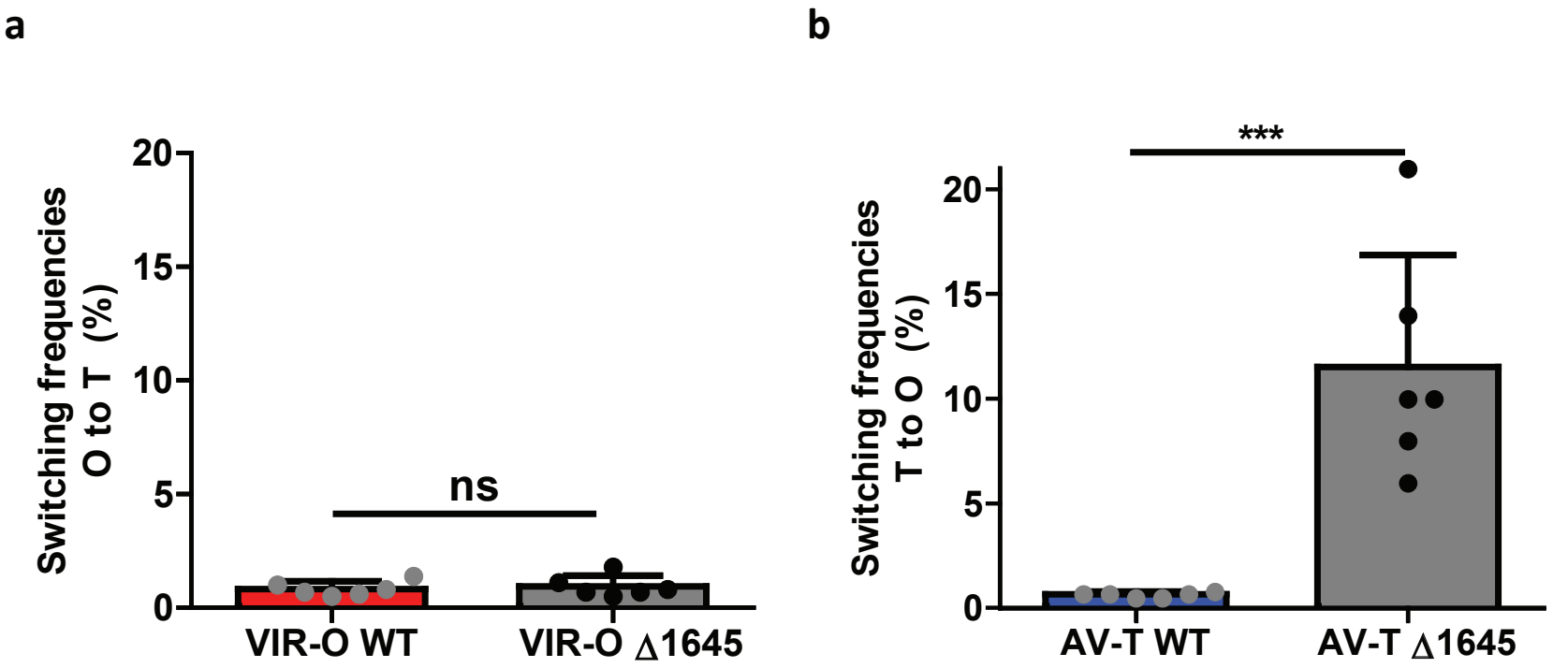

Supplementary Fig. 10. Role of ABUW_1645 in VIR-O/AV-T switching. Wild-type and isogenic *Δ1645* VIR-O and AV-T strains were serially diluted onto 0.5 X LB plates. After 20 hours of growth, well-isolated colonies (n = 6 for each) were resuspended in LB broth and serial dilutions were plated on 0.5X LB agar. The frequency of **(a)** VIR-O and **(b)** AV-T colonies was determined under stereo microscopy with oblique lighting. Error bars represent standard deviation of the mean and significance was determined using the Student's two-tailed *t*-test (***$p < 0.0005$; ns = not significant).

Supplementary Figure 11

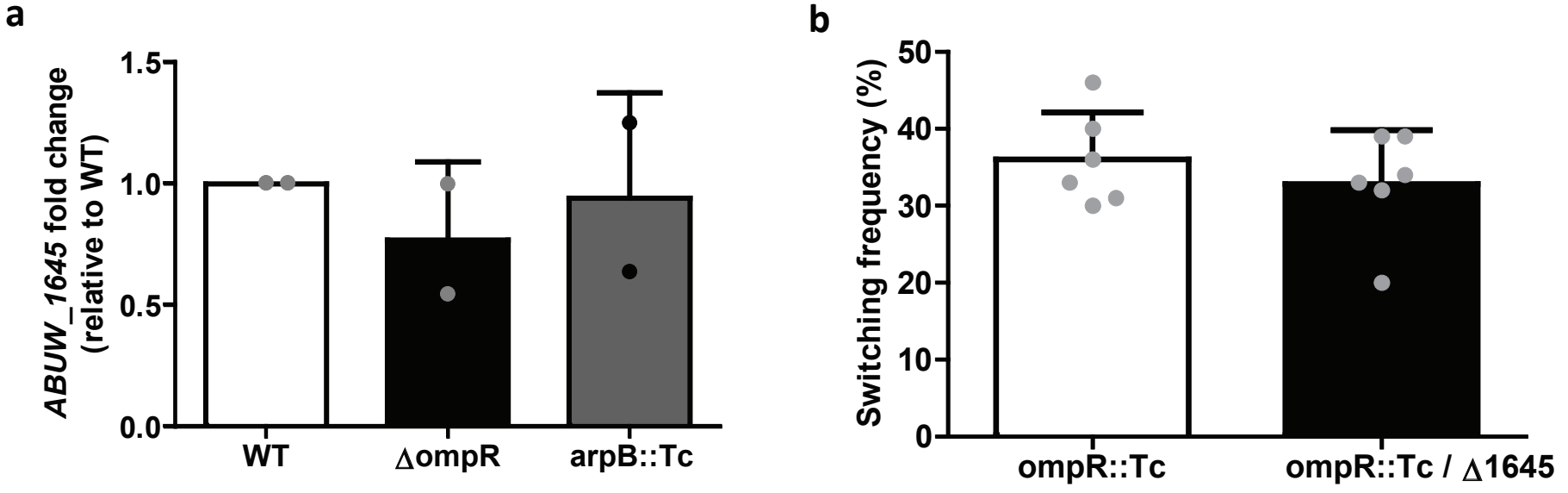

Supplementary Fig. 11. OmpR, ArpB and ABUW_1645 regulate VIR-O to AV-T switching by separate pathways. (a) qRT-PCR analysis of *ABUW_1645* expression in wild-type, *ΔompR* and an *arpB::Tc* mutant is shown. Values were determined using *clpX* as an internal control and the *ΔompR* and *arpB::Tc* values are normalized relative to wild-type. Data represents two replicates. **(b)** Frequency of switching in 24 hour colonies from VIR-O to AV-T is shown for six replicate colonies. For **(a, b)** error bars represent standard deviation of the mean.

Supplementary Figure 12

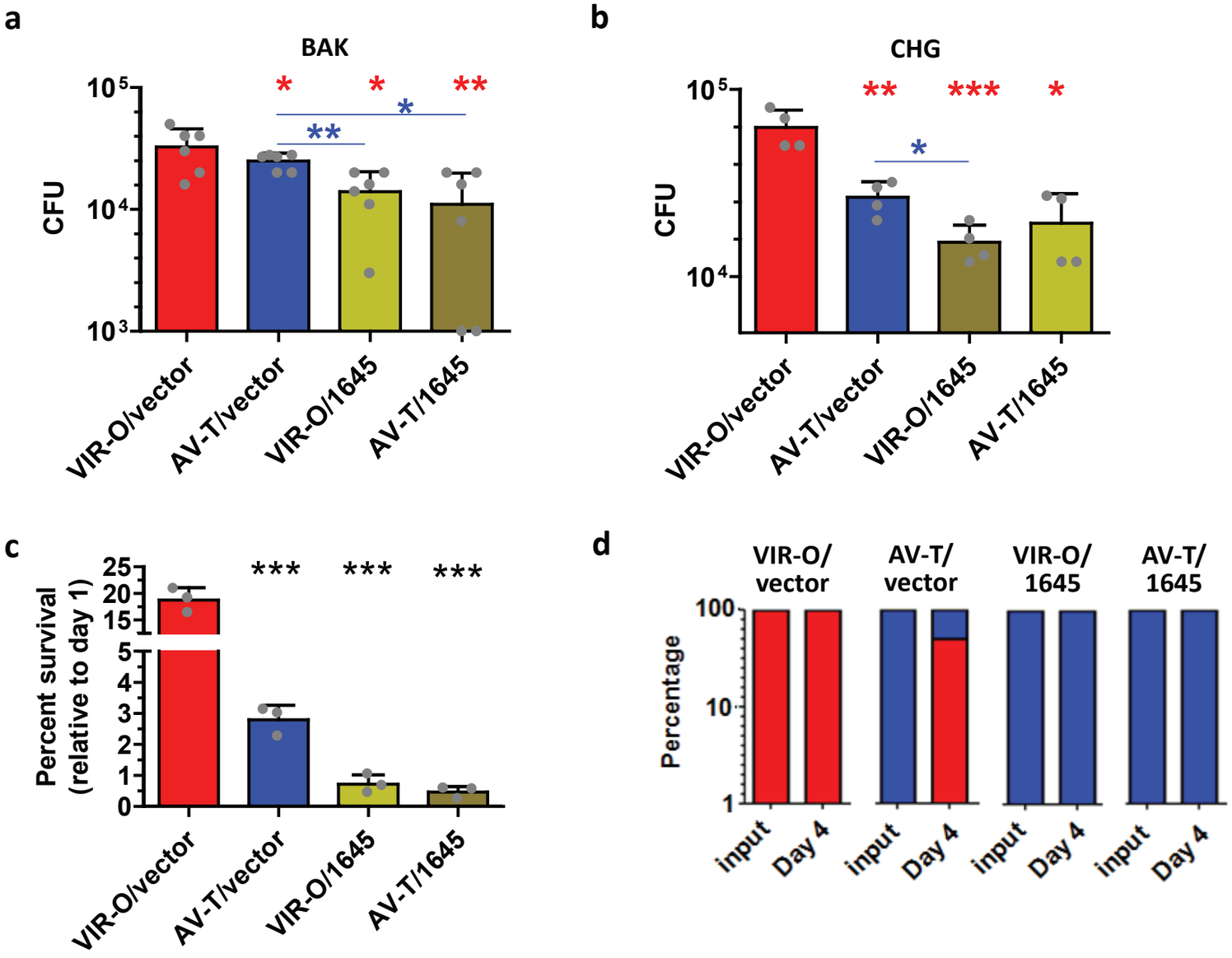

Supplementary Fig. 12. VIR-O/1645 is sensitive to desiccation and hospital-used disinfectants. (a, **b),** VIR-O/vector (red), AV-T/vector (blue), VIR-O/1645 (green) or AV-T/1645 (gold) strains was treated with the indicated amounts of disinfectants: **(a)** BAK 0.004% and **(b)** CHG 0.008%, and CFU was enumerated. Values were determined using 6 replicates for **(a)**, and four replicates for **(b)**. **(c, d)**, VIR-O/vector (red), AV-T/vector (blue), VIR-O/1645 (green) or AV-T/1645 (gold) strains was subjected for desiccation assays. **(c)**, Bacteria were rehydrated and plated on day 4 of desiccation to determine viability. Values were determined using three replicates. **(d)**, Recovered bacterial from each cells were assessed for the percentage of VIR-O and AV-T cells present (n= 3 to 5/ condition). For the above experiments, error bars represent standard deviation of the mean. *p*-values were determined using the Student's two-tailed *t*-test (*$p < 0.05$; **$p < 0.005$; ***$p < 0.0005$). Red and blue asterisks denote significance statistical analysis compared to VIR-O/vector and AV-T/vector, respectively.

Supplementary Figure 13

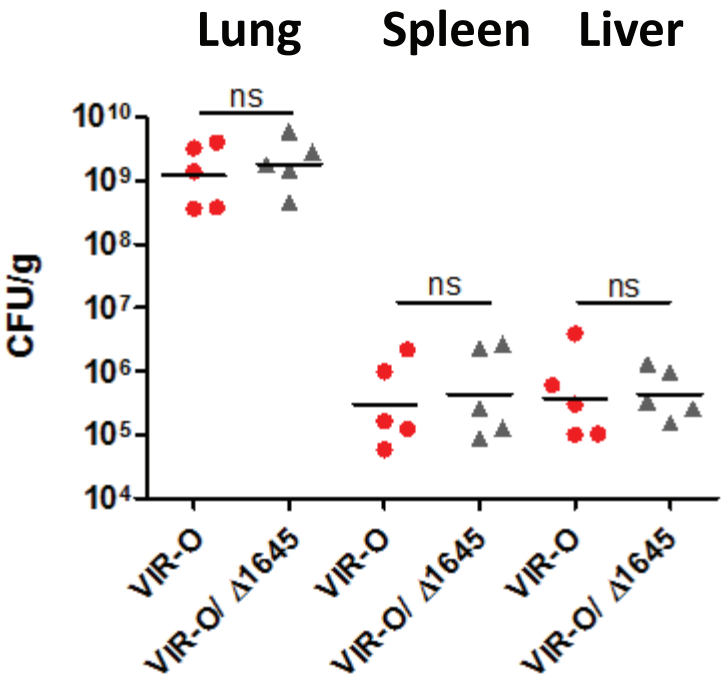

Supplementary Fig. 13. ABUW_1645 is not required for virulence in a lung model of infection. Mice were infected intranasally with VIR-O (red) or VIR-O *Δ1645* (gray) strains (n=5/ group). At 24 hours post-infection, organs were harvested and plated for colony forming unit enumeration. Error bars represent geometric mean and significance was determined using a two-tailed Mann-Whitney test (ns= not significant).

Supplementary Table S1. Differentially expressed genes between the VIR-O and AV-T cells.
ABUW_1645 regulated genes are highlighted in blue. Data was compiled from three biological replicates for each condition. The Fisher's Exact Test (modified by DESeq) was used to calculate the *p*-values, which were adjusted for multiple-testing with the Benjamini-Hochberg method.